

Summary

- We present a novel whole brain analytics and simulation method.
- Deep-learning based causality analysis significantly outperforms conventional analytics methods such as Functional Connectivity, multivariate Granger Causality, and Transfer Entropy in the large node case.

Abstract

To elucidate brain function and pursue pathological studies, the development of in silico simulation offers a number of opportunities to study the properties of the brain in a non-invasive manner. In this study, we use a data driven method to analyze the causal relationship between non-linear input and output, and we evaluate its performance over a number of aspects. Our model comprises a fully connected network where each node is a deep neural network. The weights within and between nodes can be trained on multi-modal data, such as *fMRI BOLD*, calcium imaging, etc., and our model can be easily expanded to large-scale simulation.

Methods

Deep-Learning based Causal Model (DLCM)

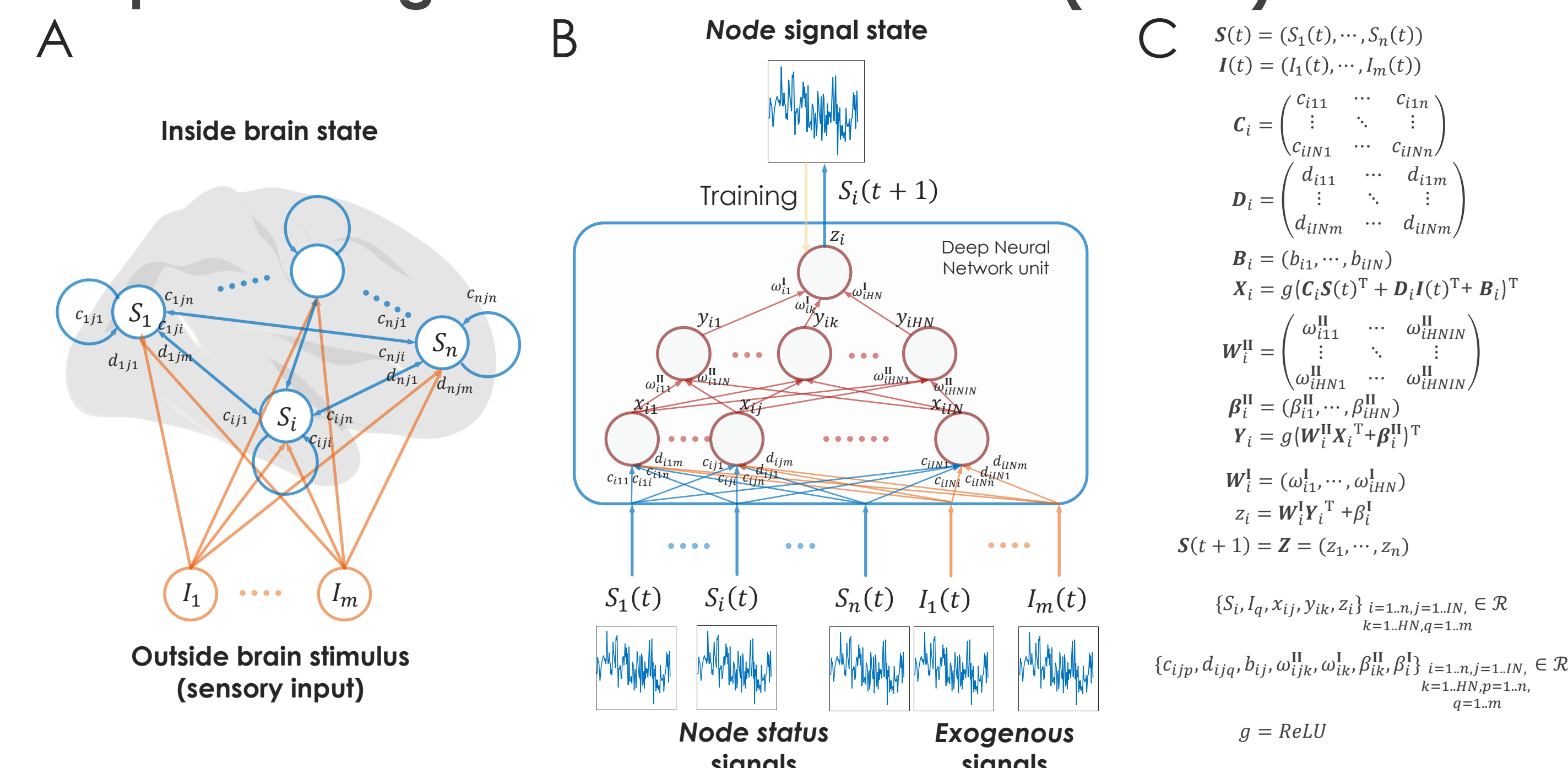


Figure 1. Definition of Deep-Learning based Causal Model

(A) Whole brain node status network and stimulus coming from outside brain (mainly sensory input) (B) Showing signaling framework of one node status. A Deep Neural Network (DNN) node receives the signal state of other brain nodes and exogenous signals (outside brain stimulus). DNN unit calculates one output signal, in this case the next time step of the signal state of a node. A DNN unit is trained by teacher signals and the input of other node states and exogenous signals. (C) The mathematical expression of Deep-Learning based Causal Model.

DLCM Granger Causality (DLCM-GC)

Granger Causality (GC)[1] is a well established analytics method for time series and multivariate GC (mvGC)[2] is applied for analyzing *fMRI BOLD* signals. If $\mathbf{S}(t)$ is the node vector $(S_1(t), \dots, S_n(t))$ and each node S_i has time series of $\{S_i(1), \dots, S_i(L)\}$. $S_i(t)$ is expressed by time lag p , the coefficient vector \mathbf{A}_{ik} and a residual $\varepsilon_i(t)$:

$$S_i(t) = \sum_{k=1}^p \mathbf{A}_{ik} \mathbf{S}(t-k)^T + \varepsilon_i(t) \quad (1)$$

If node j relation is removed from node i ,

$$S_i^{(-j)}(t) = \sum_{k=1}^p \mathbf{A}_{ik}^{(-j)} \mathbf{S}^{(-j)}(t-k)^T + \varepsilon_i^{(-j)}(t) \quad (2)$$

the mvGC of $S_{j \rightarrow i}$ is expressed by

$$S_{j \rightarrow i} = \log \left(\frac{\text{var}(\varepsilon_i^{(-j)})}{\text{var}(\varepsilon_i)} \right) \quad (3)$$

where ε_i and $\varepsilon_i^{(-j)}$ are time series of residuals, $\text{var}()$ denotes the statistical variance. For mvGC the coefficients and residuals are calculated by linear regression. Recently, Neural Network based Granger Causality is studied in several literatures, such as NN-GC [3], RNN-GC [4], ES-GC [5] and DNN-GC [6]. DLMC can also calculate this type of Granger Causality. We simply use $\text{Err}_i = \mathbf{S}_i - \text{Teach}_i$ of single node i as residuals ε_i and removing signal from node j , $\text{Err}_i^{(-j)} = \mathbf{S}_i^{(-j)} - \text{Teach}_i$ as residuals $\varepsilon_i^{(-j)}$. Then, DLMC-GC is defined

$$S_{j \rightarrow i} = \log \left(\frac{\text{var}(\text{Err}_i^{(-j)})}{\text{var}(\text{Err}_i)} \right) \quad (4)$$

Importantly, removing the signal from another node can be thought of as lesion simulation. One brain region is virtually impaired and expressed as Granger Causality. Therefore, DLMC can also work as a lesion model [7].

Results

DLCM is trained by fully random signals

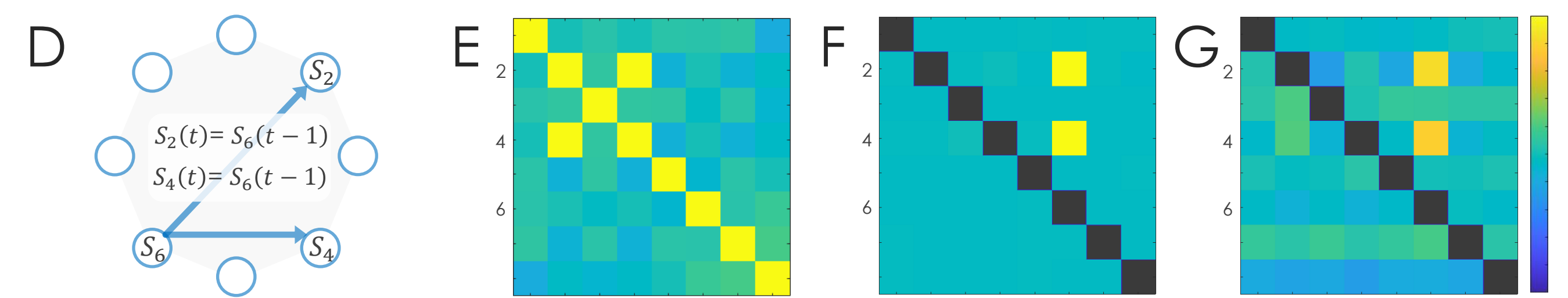
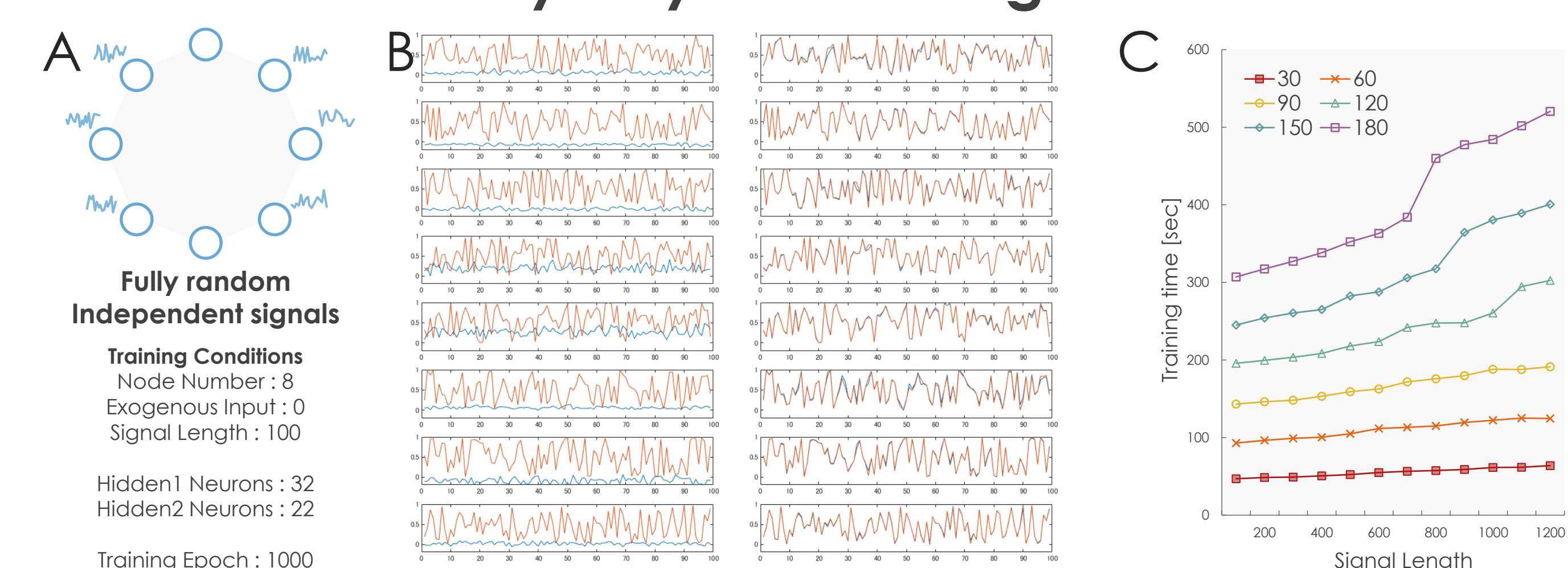


Figure 2. Training result of fully random (uniform distribution) signals

(A) Node network image and training conditions. (B) Left shows before training signals of 8 nodes (Red: teaching signal, Blue: DLMC output). Right shows after training signals. Left Mean Absolute Error (MAE) is 0.456. Right MAE is 0.018. DLMC was successfully trained. (C) Training time result of signal length and node count. (D) Node network image for evaluating Functional Connectivity (FC), mvGC and DLMC-GC. Node 6 signal is copied to node 2 and 4 at next time step. (E) FC result of D. Color range is [-1, 1]. (F) mvGC result of D. Color range is [-5σ, 5σ]. (G) DLMC-GC result of D. Color range is [-5σ, 5σ].

DLCM-GC can detect network connections from DCM simulated BOLD signals as well as mvGC, etc.

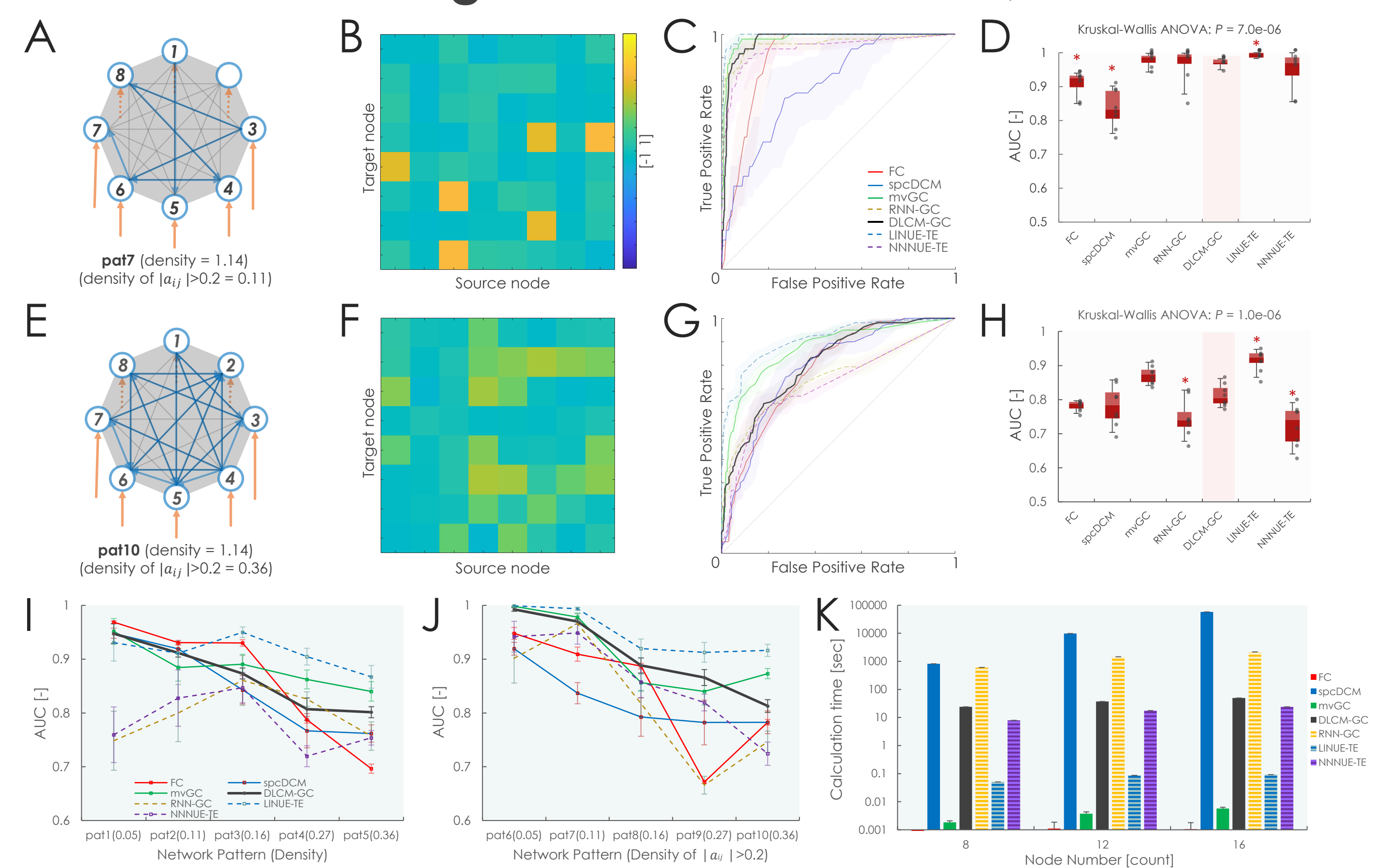


Figure 3. Evaluation result of 7 algorithms to detect ground truth connections

(A) Node network image pat7 - all nodes were connected and some nodes had strong connections. (B) Adjacency matrix \mathbf{A} of network in A, used by Spectral DCM (spcDCM) [8]. This provides a ground truth connectivity for the DCM and 8 node signals were generated together with 8 exogenous signals. (C) ROC curve of detecting ground truth matrix, (strong connection: $|a_{ij}| > 0.2$). Seven algorithms were compared: FC, spcDCM, mvGC, RNN-GC, DLMC-GC, LINUE-TE (Transfer Entropy) and NNNUE-TE. (D) AUC of C, Steel test: $* P < 0.05$. (E) Node network image of pat10. (F) Adjacency matrix \mathbf{A} of network in E. (G) ROC curve of detecting ground truth in F. (H) AUC of G. (I) Network density (sparse pattern) vs. AUC result. (J) Network density (fully connected) vs. AUC result. (K) Computation time results. spcDCM was calculated by DCM12 on MATLAB 2019b. LINUE-TE and NNNUE-TE were calculated by MuTE [9] on MATLAB. RNN-GC was calculated using Python 3.6. Machine spec was OS: Windows 10 Pro; CPU: AMD Ryzen Threadripper 3970X 32-Core Processor 3.70GHz, Mem:128GB. Tested node counts were 8, 12 and 16 and number of trials were spcDCM N=20,10,4 (due to large computation time) and all others N=20,10,10.

DLCM-GC significantly outperforms mvGC and LINUE-TE in large node case

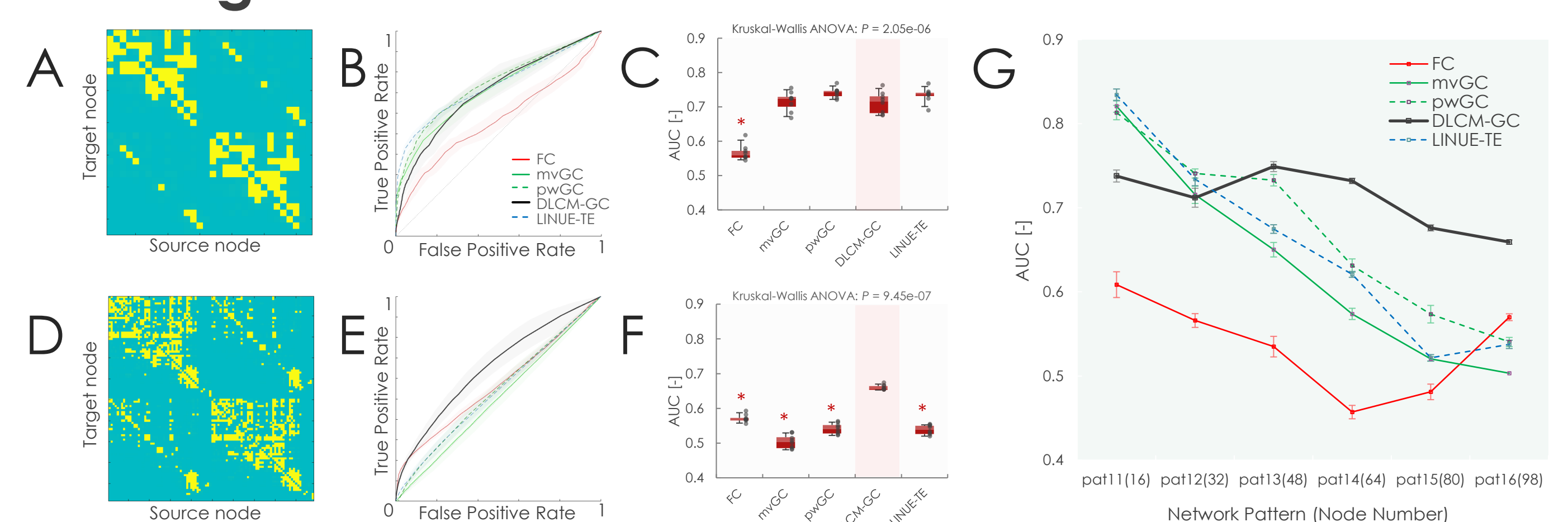


Figure 4. Evaluation result of 5 algorithms to detect original connections.

(A) Ground truth connectome matrix \mathbf{C} (pat12(32)) for generating node signals calculated by the reduced wong-wang model [10] from The Virtual Brain software [11]. Matrices were generated from Allen's mouse connectome matrix [12][13]. Node numbers were 16,32,48,64,80,98 and all network densities ($|c_{ij}| > 1$) were 0.15. (B) ROC curve of detecting ground truth matrix \mathbf{C} . 5 algorithms, FC, mvGC, pwGC, DLMC-GC, LINUE-TE were compared. (C) AUC of B, Steel test: $* P < 0.05$. (D) Ground truth connectome matrix \mathbf{D} (pat16(98)) (E) ROC curve of detecting ground truth matrix \mathbf{D} . (F) AUC of E. (G) AUC results for different node numbers.

Acknowledgement

This research was supported by the program for Brain Mapping by Integrated Neurotechnologies for Disease Studies (Brain/MINDS) from the Japan Agency for Medical Research and Development, AMED. Grant number: JP20dm0207001.

References

- Granger, C.W.J. (1969) *Econometrica* 37 (3), 424-438.
- Goebel, R et al. (2003) *Mag.Res.Imaging* 21, 1251-1261.
- Montalto, A et al. (2015) *Neural Netf.* 71, 159-171.
- Wang, Y et al. (2018) *IEEE Trans.Bio.Eng.* 65 (9), 1953-1963.
- Duggento, A et al. (2019) *bioRxiv*, 651679.
- Chivukula, A.S et al. (2018) *Advances A.I.*, 692-705.
- Honey, C.J et al. (2008) *H.BRAIN MAP.* 29 (7), 802-809.
- Friston, K et al. (2013) *NeuroImage* 94, 396-407.
- Montalto, A et al. (2014) *PLoS ONE* 9(10), e109462.
- Wong, K.F et al. (2006) *J.Neuroscience* 26(4), 1314-1328.
- Leon, P.S et al. (2013) *Front. Neuroinform.* 7:10.
- Oh, S.W et al. (2014) *Nature* 508, 207-214.
- Melozzi, F et al. (2017) *eNeuro* 4 (3) ENEURO.0111-17.2017.